1993

Onset of spatially chaotic waves on flowing films

Jun Liu

Jerry P. Gollub
Haverford College

Repository Citation

Liu, Jun, and Jerry P. Gollub. "Onset of spatially chaotic waves on flowing films." Physical review letters 70.15 (1993): 2289-2292.

Onset of Spatially Chaotic Waves on Flowing Films

Jun Liu and J. P. Gollub
Physics Department, Haverford College, Haverford, Pennsylvania 19041
and Physics Department, University of Pennsylvania, Philadelphia, Pennsylvania 19104
(Received 14 January 1993)

Periodic two-dimensional waves on the surface of a flowing film are generally unstable. We have investigated their breakdown experimentally to determine the process by which film flows undergo a transition to spatiotemporal chaos. The two-dimensional secondary instabilities studied here are convective (like the primary instability); both subharmonic and sideband instabilities occur, but in different ranges of frequency.

PACS numbers: 47.35.+i, 47.20.Lz, 47.52.+j

The onset and development of spatiotemporal chaos has recently been investigated in various nonlinear systems. Examples have been found in hydrodynamic, chemical, and optical systems, among others [1]. Quantitative studies of the processes leading to space-time disorder are still limited, though defect generation and symmetry-breaking instabilities seem to be widespread in some of the examples. A unified theoretical approach to these phenomena is still lacking.

Thin liquid films flowing down an incline provide a useful context for exploring the development of spatiotemporal chaos in open-flow systems, which typically exhibit *convective instability* [2,3]. In these systems, disturbances are amplified only in a comoving frame of reference. This type of instability has been characterized in several recent experiments [4]. Flowing films are unstable to sufficiently long waves [5] when the Reynolds number is above its critical value $R_c = \frac{5}{4}\cot\beta$. Here β is the inclination angle that the film plane makes with the horizontal; the Reynolds number $R = u_0 h_0/\nu$ is based on the unperturbed film thickness h_0, the fluid velocity u_0 at the surface, and the kinematic viscosity ν. The initial instability is convective and the resulting waves are said to be *noise sustained,* i.e., sensitive to noise at the source [3,6].

The nonlinear evolution of these waves depends strongly on their initial frequency f [6,7] as determined by small amplitude forcing near the inlet. Two types of nonlinear evolution are found: Saturated finite amplitude waves occur at high frequency, and solitary waves (generally composed of a large maximum and several subsidiary peaks) dominate at low frequency. At a sufficiently large distance downstream, complex disordered patterns develop and the waves eventually become statistically independent of perturbations near the source. However, the processes leading to disordered waves are not understood.

Theoretical modeling of wavy film flows has a long history. For large surface tension, the widely studied Kuramoto-Sivashinsky (KS) equation is applicable to waves in film flows close to R_c. Chang, Demekhin, and Kopelevich [8] showed that even for larger R model equations suitable for describing nonlinear waves have behavior close to that of the KS equation. Sideband instability [9] and subharmonic instability [10] occur in this and other wave systems. For film flows, different theoretical methods lead to apparently different conclusions concerning the importance of the Eckhaus sideband instability [11]. Several authors have discussed the existence of subharmonic instability [12]; Chang, Demekhin, and Kopelevich [8] argued that both sideband and subharmonic instabilities can occur in different frequency regimes.

Experimental studies of the secondary instability of film flows are limited. Alekseenko, Nakoryakov, and Pokusaev found [7] that waves in some ranges of frequency are unstable. The experiments of Brauner and Maron [13] suggest that spatial period doubling may occur in film flows, but the process was not studied quantitatively.

In this Letter, we report experiments on the *secondary two-dimensional instability* of periodic waves, in order to explore the means by which these waves become disordered. We find that both subharmonic and sideband instabilities occur, but in different ranges of frequency: *Sideband instability* predominates for high frequency waves while *subharmonic instability* appears at lower frequency. These instabilities initiate complicated coalescence and splitting processes of wave fronts, and lead to one-dimensional spatiotemporal chaos, provided that the viscosity is sufficient to suppress three-dimensional instability.

The flow and measurement systems are briefly described as follows; a detailed description can be found in Ref. [6]. The film plane is 200 cm long by 50 cm transverse to the flow; relatively small inclination angles from 6° to 10° are employed. The entrance flow rate is perturbed at frequency f and amplitude A by applying small pressure variations to the entrance manifold under computer control. Aqueous solutions of glycerin (54% by weight) are used in this experiment; the kinematic viscosity and surface tension are 6.16 cS (centistokes) and 67 dyn/cm at 22.5 °C. The working temperature varies by less than 0.4 °C. We use a fluorescence imaging method to measure the film thickness $h(x,y,t)$ in real time with a sensitivity of 8–10 μm. We also measure the local wave slope $s(x_0,t)$ by laser beam deflection. This signal is superior for computation of spectra; its sensitivity of

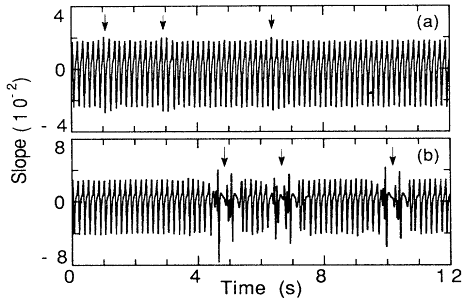

FIG. 1. Instability of periodic waves to small pulse modulations of the forcing amplitude, at (a) $x=28$ cm and (b) 92 cm. The extreme instability of the waves is evident, along with the *convective* character of this instability. The Reynolds number is $R=18$, the inclination angle is $\beta=7.4°$, and the wave frequency is $f_0=6$ Hz.

5×10^{-5} corresponds typically to wave amplitudes of 0.5 μm.

In Fig. 1 we show simultaneous wave slope data at two positions to illustrate the response of periodic waves to small perturbations. Sinusoidal forcing is first applied at the entrance. Periodic waves grow downstream and saturate at a sufficient distance from the source. Three small pulselike modulations of forcing amplitude are then applied at uneven intervals. At $x=28$ cm from the source [Fig. 1(a)], we see three small humps (arrows) on the periodic waves. The modulations grow only in a comoving frame of reference. At $x=92$ cm, they have developed into complicated localized waves [Fig. 1(b)] that are eventually convected out of the system; the periodic waves resume after passage of the modulations. *This observation demonstrates that periodic waves are convectively unstable.*

Each localized pulse [Fig. 1(b)] consists mainly of several near-solitary waves with large humps and subsidiary peaks. These complex local structures are generated primarily by nonlinear wave dynamics, and not by linear amplification of high frequency components of the modulations. The applied perturbations *initiate* the transition to turbulence although the transition itself is a nonlinear process [3]. Disorder can also be initiated by *natural noise.*

We find that periodic waves are unstable over a wide frequency band with respect to subharmonic instability. An example is given in Fig. 2(a) for $\beta=6.4°$, which shows the spatiotemporal evolution of the film thickness in a section 43 cm long in the streamwise direction. Periodic waves ($f_0=7.2$ Hz) generated at the entrance are found to saturate roughly at $x=55$ cm. Slight modulation of the wavelength is visible at $x=80$ cm and is amplified downstream. When the spacing between two adjacent troughs increases, the neighboring spacing decreases. The waves then coalesce in pairs as they travel, and therefore the period is roughly doubled. It is evident that *the period doubling is irregular both in space and in time.*

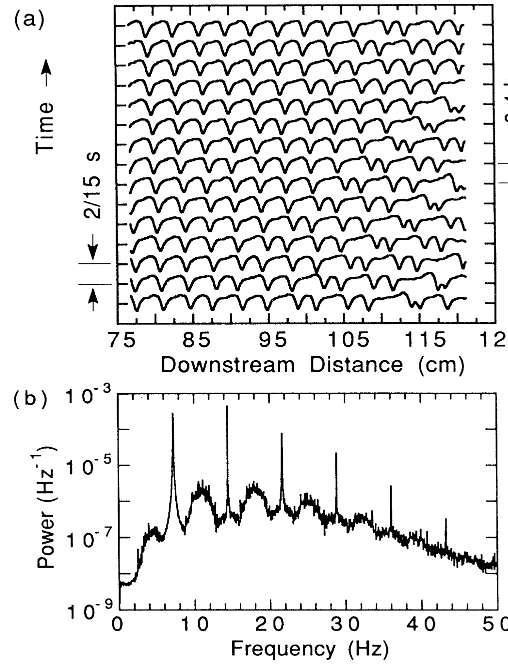

FIG. 2. (a) Space-time evolution of the film thickness, showing the spontaneous subharmonic instability of periodic waves. The wave profiles are shown at time intervals of $\frac{2}{15}$ s; the amplitude scale is shown at the right. (b) Corresponding power spectrum of the local wave slope at $x=77$ cm ($f_0=7.2$ Hz, $R=34$, $\beta=6.4°$).

The power spectra of the local wave slope at $x=77$ cm [Fig. 2(b)] show that broad spectral peaks appear at $f=(n+\frac{1}{2})f_0$ where n is an integer. (The sharp peaks are located at multiples of the forcing frequency.) This behavior is consistent with the apparent spatial period doubling, though the $f_0/2$ peak is relatively weak. There is no evidence of successive spatial period doubling. Waves at lower frequency are less unstable to the subhar-

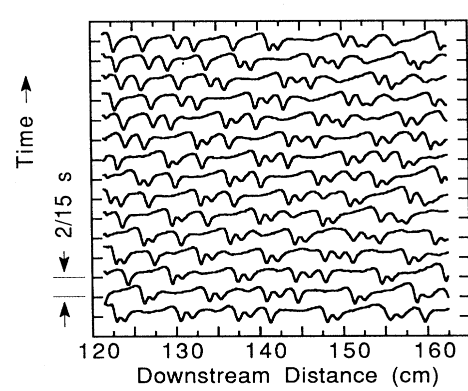

FIG. 3. Spatiotemporal chaos due to subharmonic instability at $f_0=7.2$ Hz ($\beta=6.4°$, $R=34$).

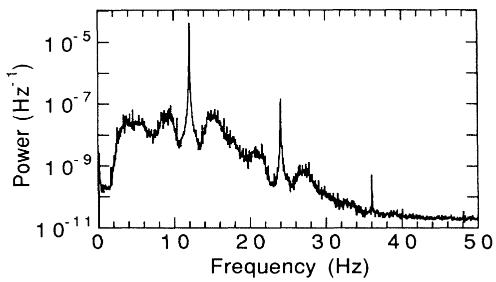

FIG. 4. Power spectrum showing sideband instability at a higher wave frequency $f_0=12$ Hz ($x=77$ cm, $\beta=6.4°$, $R=34$).

monic instability, though the addition of weak broadband noise at the entrance causes the subharmonic peaks to appear even at low f_0. This convective subharmonic instability initiates complicated coalescence and splitting processes of the wave fronts, and leads to one-dimensional spatiotemporal chaos downstream, as shown in Fig. 3.

When the wave frequency is large enough (a stability boundary is given later), chaotic flows develop *without* spatial period doubling. Figure 4 shows an example where the fundamental frequency is $f_0=12$ Hz and other conditions are the same as those in Fig. 2. Amplified low frequency noise (presumably external) is found in a broad band near 4 Hz *even without periodic forcing.* When the forcing is added, the noise interacts with the main wave peaks to produce sidebands around each main peak. Further downstream complicated coalescence and splitting processes lead to irregular trains of (nearly) solitary waves. We refer to this process as a sideband instability, but it is quite different from the Eckhaus mechanism.

To study the growth rates of the secondary instabilities, we use *two frequency forcing.* A small perturbation at f_1 is superposed on f_0, with a power ratio of 10^{-3}. We measure the ratio of the spectral power (at frequency f_1) at two downstream positions (x_1 and x_2) to determine the average dimensionless growth rate σ of perturbations,

$$\sigma(f_1)=\frac{h_0}{2(x_2-x_1)}\ln\frac{P(x_2,f_1)}{P(x_1,f_1)},$$

where $P(x,f)$ is the power spectral density at position x and frequency f. Figure 5 gives the result as a function of the frequency ratio f_1/f_0 for two different values of f_0. At $f_0=7.2$ Hz, there is a sharp though modest resonance peak at the subharmonic frequency, $f_1/f_0=0.5$. However, the growth rate also shows a broad hump around the subharmonic frequency. This behavior is consistent with the existence of broad subharmonic peaks in the power spectrum [Fig. 2(b)]. On the other hand, when $f_0=12$ Hz, the subharmonic resonance disappears and the maximum growth rate occurs around $f_1/f_0=0.4$, a value that is close to the frequency of maximum growth (4.3 Hz) predicted by linear theory for these conditions. The aver-

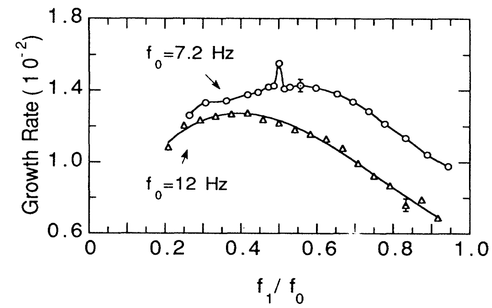

FIG. 5. Average spatial growth rate of perturbations at frequency f_1 to waves at frequency f_0, as a function of f_1/f_0. The subharmonic resonance is present when $f_0=7.2$ Hz, but not at 12 Hz ($\beta=6.4°$, $R=34$).

age growth rates at frequency $f_0\pm f_1$ show the same behavior.

The boundary separating the sideband and subharmonic secondary instabilities is shown in the phase diagram of Fig. 6 ($\beta=6.4°$). The solid and dashed lines $f_c(R)$ and $f_m(R)$ give the neutral stability curve for the primary wave onset and the most amplified wave frequency, both of which have been confirmed experimentally [6]. Periodic waves appear to be unstable at least from f_c down to f_m. Sideband instability of the primary waves predominates near f_c, and subharmonic instability at lower frequencies. The dividing line between these two mechanisms is given by the squares. Because of the finite length of the film plane, it is difficult to study the secondary instabilities of the primary waves at frequencies lower then f_m. At very low frequencies, the development of disorder is quite different; the solitary wave spacing is so large that new waves develop independently between them [6]. Our results suggest that the lower boundary of subharmonic instability is close to $f_m(R)$ and may be lower than f_m for large R.

At the present time there is no theory with which we can compare these results quantitatively. On the other hand, the general behavior observed here, with sideband instability close to f_c and subharmonic instability at lower frequencies, appears to be consistent with the theoretical approach of Ref. [8]. It is clear that the

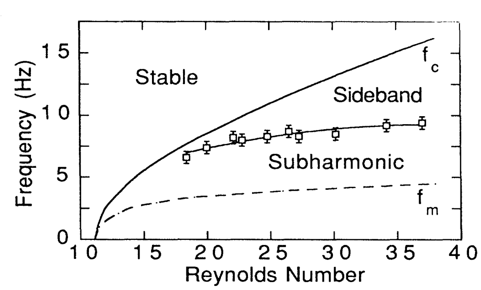

FIG. 6. Stability boundaries showing the different character of the secondary instability as a function of f and R (see text).

specific sideband mechanism discussed by Eckhaus and by Benjamin and Feir [9], which involves higher order nonlinear interactions than those we observe, is not prominent here. At lower viscosity, three-dimensional instabilities are found in which the wave fronts become deformed in the cross-stream direction; these instabilities will be the subject of a future publication, and have been studied theoretically in the case of a vertical film [14].

We have demonstrated that the transition to spatiotemporal chaos in one space dimension (and time) involves distinct two-dimensional secondary instabilities that dominate in different ranges of frequency. We show that the *secondary* instability is convective and hence sensitive to noise, as anticipated by Deissler in numerical studies of model equations for open flow systems [15]. Film flow instabilities have many features in common with other shear flows, so that behavior studied here under relatively ideal conditions may have analogs in these systems as well.

We appreciate helpful discussions with H.-C. Chang, R. E. Kelly, M. Sangalli, and M. Cheng. The work was supported by NSF Grant No. CTS-9115005.

[1] For a review, see M. C. Cross and P. C. Hohenberg, Rev. Mod. Phys. (to be published); M. Caponeri and S. Ciliberto, Physica (Amsterdam) **58D**, 365 (1992).

[2] P. Huerre and P. A. Monkewitz, Annu. Rev. Fluid Mech. **22**, 473 (1990).

[3] R. J. Deissler, Physica (Amsterdam) **25D**, 233 (1987).

[4] E.g., K. L. Babcock, G. Ahlers, and D. S. Cannell, Phys. Rev. Lett. **67**, 3388 (1991); M. F. Schatz, R. P. Tagg, and H. L. Swinney, Phys. Rev. Lett. **66**, 1579 (1991); V. Steinberg and A. Tsameret, Phys. Rev. Lett. **67**, 3392 (1991).

[5] C. S. Yih, Phys. Fluids **6**, 321 (1963); T. B. Benjamin, J. Fluid Mech. **2**, 554 (1957).

[6] J. Liu, J. D. Paul, and J. P. Gollub, J. Fluid Mech. (to be published), and references therein.

[7] S. V. Alekseenko, V. Y. Nakoryakov, and B. G. Pokusaev, AIChE J. **31**, 1446 (1985).

[8] H.-C. Chang, E. A. Demekhin, and D. I. Kopelevich, J. Fluid Mech. (to be published).

[9] W. Eckhaus, *Studies in Nonlinear Stability Theory* (Springer, Berlin, 1965); T. B. Benjamin and J. E. Feir, J. Fluid Mech. **27**, 417 (1967).

[10] R. E. Kelly, J. Fluid Mech. **27**, 657 (1967).

[11] S. P. Lin, J. Fluid Mech. **63**, 417 (1974); M. Cheng and H.-C. Chang, Chem. Eng. Commun. **118**, 327 (1992).

[12] T. Prokopiou, M. Cheng, and H.-C. Chang, J. Fluid Mech. **222**, 665 (1991); S. W. Joo and S. H. Davis, Chem. Eng. Commun. **118**, 111 (1992).

[13] N. Brauner and D. M. Maron, Int. J. Heat Mass Transfer **25**, 99 (1982).

[14] S. W. Joo and S. H. Davis, J. Fluid Mech. **242**, 529 (1992).

[15] R. J. Deissler, J. Stat. Phys. **54**, 1459 (1989).